BEST AVAILABLE IMAGES

Defective images within this document are accurate representations of the original documents submitted by the applicant.

Defects in the images may include (but are not limited to):

- BLACK BORDERS
- TEXT CUT OFF AT TOP, BOTTOM OR SIDES
- FADED TEXT
- ILLEGIBLE TEXT
- SKEWED/SLANTED IMAGES
- COLORED PHOTOS
- BLACK OR VERY BLACK AND WHITE DARK PHOTOS
- GRAY SCALE DOCUMENTS

IMAGES ARE BEST AVAILABLE COPY.

As rescanning documents *will not* correct images, please do not report the images to the Image Problem Mailbox.

4191

80

Aortic Input Impedance in Normal Man: Relationship to Pressure Wave Forms

JOSEPH P. MURGO, M.D., LTC, MC, NICO WESTERHOF, PH.D., JOHN P. GIOLMA, PH.D., CPT, MSC, AND STEPHEN A. ALTOBELLI, M.Sc., ILT, SIGC

SUMMARY The relationship between the shape of the ascending aortic pressure wave form and aortic input impedance was studied in 18 patients who underwent elective cardiac catheterization but in whom no heart disease was found. Ascending aortic flow velocity and pressure were simultaneously recorded from a multisensor catheter with an electromagnetic velocity probe and a pressure sensor mounted at the same location. Another pressure sensor at the catheter tip provided left ventricular pressure or a second aortic pressure to determine pulse-wave velocity. Fick cardiac outputs were used to scale the velocity signal to instantaneous volumetric flow. Input impedance was calculated from 10 harmonics of aortic pressure and flow. For each patient, impedance moduli and phases from a minimum of 15 beats during a steady state were averaged. Peripheral resistance was 1137 ± 39 dyn-sec-cm^{-5} (± SEM) and characteristic impedance was 47 ± 4 dyn-sec-cm^{-5}; pulse-wave velocity was 6.68 ± 0.32 m-sec^{-1}. In all patients, a well-defined systolic inflection point divided the aortic pressure wave form into an early and late systolic phase. The patients were classified into three groups: group A (n = 7) — patients whose late systolic pressure exceeded early systolic pressure; group B (n = 7) — patients whose early and late systolic pressures were nearly equal; group C (n = 4) — patients whose early systolic pressure exceeded late systolic pressure. Group A and B patients all demonstrated oscillations of the impedance moduli about the characteristic impedance. Group C patients demonstrated flatter impedance spectra. Thus, a larger secondary rise in pressure was associated with a more oscillatory impedance spectrum. These results suggest that the differences in pressure wave forms are due to differences in reflections in the arterial tree and not secondary to differences in cardiac function. Using pulse-wave velocity, the "effective" reflection site distance was determined from both pressure (48 cm) and impedance (44 cm) data, implying that the region of the terminal abdominal aorta acts as the major reflection site in normal adult man.

図9

THE CHARACTER of the arterial pulse as palpated by the physician at the bedside or displayed by laboratory pulse recording techniques has long been an important part of the clinical evaluation of the patient with heart disease. Arterial pressure is the result of an interaction between the heart and the arterial system, so that the magnitude and shape of the pressure pulse will be affected by changes in the peripheral circulation or alterations in cardiac function. Recent improvements in intravascular pressure measurement techniques have revealed major differences in the configuration of aortic pressure waves among patients, even in the absence of cardiovascular disease.[1] One way to determine whether these observations are secondary to differences in cardiac function or differences in the periphery is to use methods that selectively describe the arterial system. To do so, special relationships involving both pressure and flow must be developed. The best known of these relationships is the input impedance. In general, impedance is calculated from the ratio of the pressure difference across the system under study and the total flow through that system. The description of the arterial system found by only taking the ratio between mean pressure difference and mean flow is limited and only gives the value of peripheral resistance. The calculation of input impedance requires measuring pulsatile pressure and flow waves and deriving their respective sinusoidal components by Fourier analysis.[2, 3]

Until recently, technically adequate simultaneous pulsatile pressure and flow signals from the same location in the ascending aorta of intact, unanesthetized man have been difficult to obtain. Accordingly, few studies of ascending aortic input impedance in man have been performed and have been principally limited to patients with disease.[4-9] Furthermore, cardiologists have expressed little interest in these measurements since the derivation of impedance is complicated and its clinical usefulness has not been demonstrated. In recent years, however, pharmacologic manipulation of the systemic circulation in advanced ischemic heart disease, severe mitral and aortic regurgitation, and the congestive cardiomyopathies has stimulated an interest in more objective measurements of the arterial system[10-13] and the relationship of these measurements to ventricular load.[14, 15] The calculation of input impedance in a clinical environment has been greatly facilitated by the development of multisensor catheterization techniques[16, 17] combined with the application of dedicated minicomputers for human hemodynamic research.[18]

In this study we examined the methods to measure

From the Cardiology Service, Department of Medicine, Brooke Army Medical Center, Fort Sam Houston, Texas, and the Laboratory for Physiology, Free University, Amsterdam, The Netherlands.

Supported in part by the Scientific Affairs Division, North Atlantic Treaty Organization, NATO research grant 1595.

Presented in part at the 51st Annual Scientific Sessions of the American Heart Association, Dallas, Texas, November 15, 1978.

The opinions or assertions contained herein are the private views of the authors and are not to be construed as reflecting the views of the Department of the Army or the Department of Defense.

Address for correspondence: Joseph P. Murgo, LTC, MC, Chief of Cardiology, Department of Medicine, Brooke Army Medical Center, Fort Sam Houston, Texas 78234.

Received June 28, 1979; revision accepted December 28, 1979.
Circulation 62, No. 1, 1980.

input impedance reliably in the clinical cardiac catheterization laboratory, established the range of values of ascending aortic input impedance in normal man at rest, and investigated the relationship of impedance to the aortic pressure wave form, with particular attention to reflection phenomena.

Methods

Patients and Catheterization Techniques

Eighteen patients were catheterized for various clinical indications, the most common of which was a chest pain syndrome. No cardiovascular disease was found by hemodynamic measurements during rest and exercise, left ventricular cineangiography or coronary arteriography. All patients were studied in a basal state and were either unsedated or very lightly sedated (diazepam 10 mg orally 1 hour before the procedure). Right- and left-heart catheterizations were performed using special multisensor catheters[16, 17] during both rest and supine dynamic exercise using a bicycle ergometer. Steady-state conditions were determined by a stable heart rate and stable sequential pulmonary artery hemoglobin oxygen saturation measurements.

Oxygen consumption was then determined by collecting expired air with a Douglas bag for 5 minutes and measuring oxygen content using the Scholander technique. During the air collection, arteriovenous oxygen content difference was derived from blood specimens collected from the aorta and pulmonary artery. Cardiac output was then calculated using the direct Fick method.[19] Duplicate determinations were made to evaluate reproducibility. All hemodynamic measurements, including the pressure and flow velocity signals used to derive impedance, as described below, were recorded during this period.

Biplane left ventricular cineangiography and selective coronary arteriography were performed after hemodynamic data were collected. If the ascending aortic root was not adequately visualized during the ventriculographic study, a selective aortic root angiogram was performed to measure the mean systolic radius of the ascending aorta. The aortic radius was determined to evaluate the proximal geometry of the arterial tree. The study protocol was approved by the Clinical Investigation and Human Use Committees at Brooke Army Medical Center and the United States Army Surgeon General's Office. Informed consent was obtained from all patients.

Custom-designed left- and right-heart multisensor catheters were used. The left-heart catheter contained two solid-state pressure sensors (Millar Mikro-Tip, Millar Instruments, Houston, Texas) and an electromagnetic flow velocity probe (Carolina Medical Electronics, King, North Carolina 1973–75; Millar Instruments 1975–79). Both pressure sensors were mounted laterally, with one sensor located at the tip of the catheter and the second located 5 cm away. The catheter was designed so that the sensing electrodes of the velocity probe and the aortic pressure sensor were mounted at the same site. Using a brachial arteriotomy, this catheter was retrogradely passed across the aortic valve so that the tip sensor was within the left ventricular cavity, with the second sensor and associated electromagnetic flow velocity probe 3–5 cm above the aortic valve. This arrangement maximizes stability of the transducers in the ascending aorta while simultaneously providing left ventricular pressure. Details of the technical characteristics of these sensors, including frequency response, drift characteristics and calibration techniques, have been described.[18, 20]

Pulse-wave velocity was measured by withdrawing the catheter until both pressure transducers were in the ascending aorta. Foot-to-foot time delays[2] were measured in a minimum of 12 sequential beats using high-amplification, high-speed recordings (paper speed 1000 mm/sec). The foot-to-foot pulse-wave velocity was assumed to be equal to the phase velocity.[2, 6]

Signal Processing and Computational Techniques

The flow velocity probes were used in conjunction with either a Carolina Medical Electronics square-wave flow meter (Model 501, Carolina Medical Electronics, King, North Carolina) or a Biotronex sinewave flow meter (Model BL-613, Biotronex Laboratory, Inc., Silver Spring, Maryland). The frequency response of the flow-velocity measurements was determined primarily by the electronics with low-pass characteristics down 3 Db at 100 Hz. Pressure and flow signals were low-pass filtered with corner frequencies at 100 Hz. All data were recorded on a Honeywell 5600 analog tape recorder and an 1858 fiberoptic strip-chart recorder (fig. 1). Digital processing was obtained using a 13-bit analog-to-digital converter at 200 samples/sec coupled to a Honeywell 316 minicomputer. The technical details of the analog and digital processing have been described elsewhere.[18]

The spatial flow velocity profile in the proximal ascending aorta was assumed to be blunt[21] and cyclic changes in the diameter of the ascending aorta were considered negligible so that the aortic flow velocity signal was used to represent instantaneous volumetric flow. In vivo calibration of this signal was accomplished by integrating the area under the curves and setting those areas equal to the stroke volume as determined by the direct Fick method. Using the electrocardiographic RR interval as the fundamental period, the Fourier series of pressure and flow were determined for the first 10 harmonics. The arterial system has been shown to be sufficiently linear to permit impedance calculations.[2, 6] Arterial input impedance should be calculated from a pressure difference across the system (aortic pressure minus right atrial or venous pressure) and aortic flow. Since right atrial pressure for these patients was small compared with aortic pressure, the aortic pressure was used alone.[3] Amplitude and phase spectra of impedance were calculated by dividing amplitudes and subtracting the phase angles of the aortic pressure and flow components.

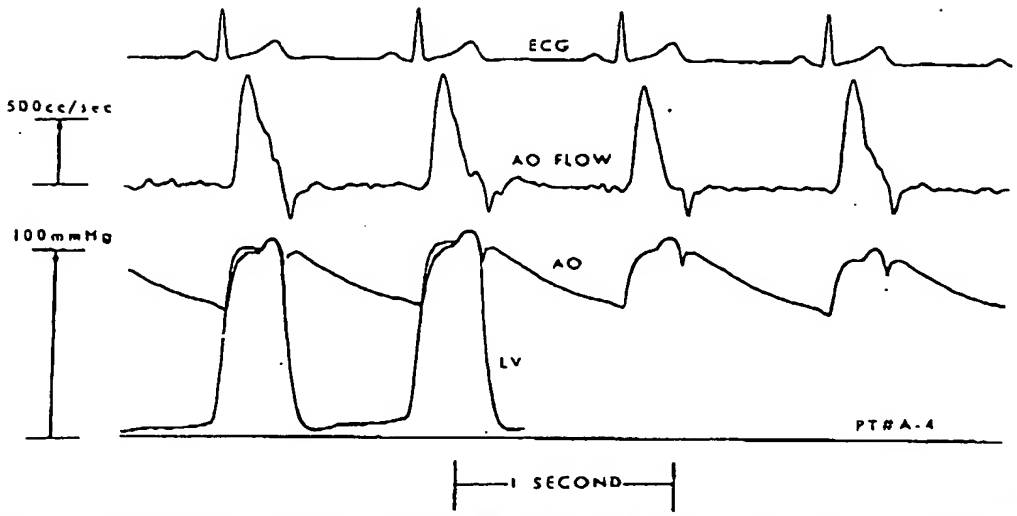

FIGURE 1. *Example of a multisensor catheter recording. AO = aortic; LV = left ventricular pressure.*

A spectral averaging algorithm was used to remove the effects of noise in the physiologic signals, especially the flow velocity signal, which inherently has a poorer signal-to-noise ratio than pressure. Those cardiac cycles with a fundamental frequency outside the range of ± 10% of the average were eliminated from the computation. At least 15 beats formed the basis of further averaging. The means and standard deviations of the impedance moduli of the remaining spectra were then calculated. All impedance moduli beyond ± 2 SD were removed in calculating a final average modulus spectrum. Means and standard deviations for the phase spectral components were also calculated, eliminating terms outside the range of ± 90 degrees up to the fifth harmonic. Beyond the fifth harmonic, an additional ± 5 degrees per harmonic were allowed because small errors in delay times produce large errors in the calculation of phase components at the higher harmonics.[3] For example, at the sixth harmonic, phase angles outside ± 95 degrees were eliminated: All phase angles beyond ± 2 SD were deleted in calculating a final average phase spectrum. This technique has the effect of removing spurious data caused by noise and by the integer arithmetic operations on very small components of flow and pressure. These procedures resulted in discarding 5–10% of the original data points. To indicate the variability of the spectra and the effects of this averaging technique, 18 spectra and their average spectrum from a single patient are shown in figure 2. Characteristic impedance was defined as the average of all impedance moduli above 2 Hz.[4]

To relate the pattern of the impedance spectral plots to the shape of the ascending aortic pressure wave form, patients were divided into three subgroups. Figure 3 illustrates the basis for this classification:

Type A: patients whose peak systolic pressure (P_{pk}) occurred in late systole after a well-defined inflection point (P_i) and $\Delta P/PP > 0.12$, where $\Delta P = P_{pk} - P_i$ and PP = total pulse pressure.

Type B: patients whose peak systolic pressure also occurred in late systole following an inflection point, but $0.0 < \Delta P/PP \leq 0.12$ (not illustrated).

Type C: patients whose peak systolic pressure preceded a well-defined inflection point and $\Delta P/PP \leq 0.0$ (i.e., a negative slope between P_{pk} and P_i).

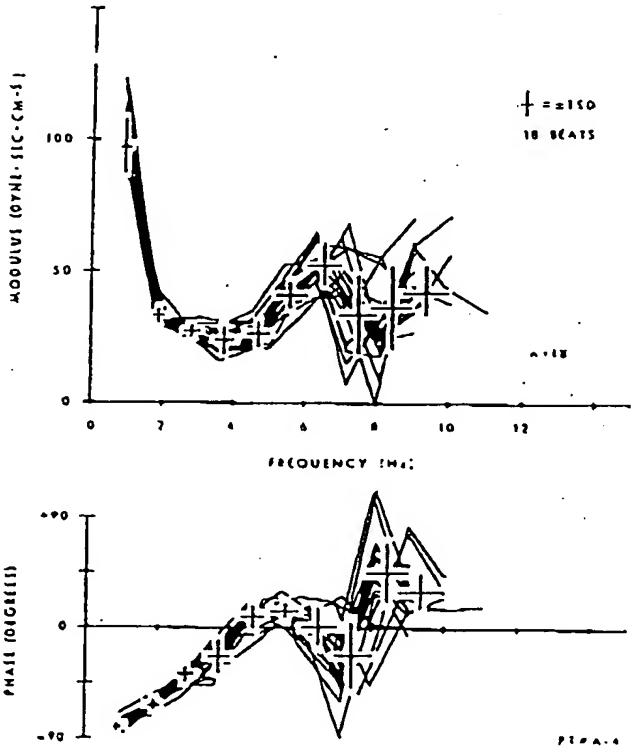

FIGURE 2. *Example of arterial input impedance computed from 18 beats and the calculated average impedance. The zero-Hz term of the impedance is 1066 ± 67 dyn-sec-cm⁻⁵.*

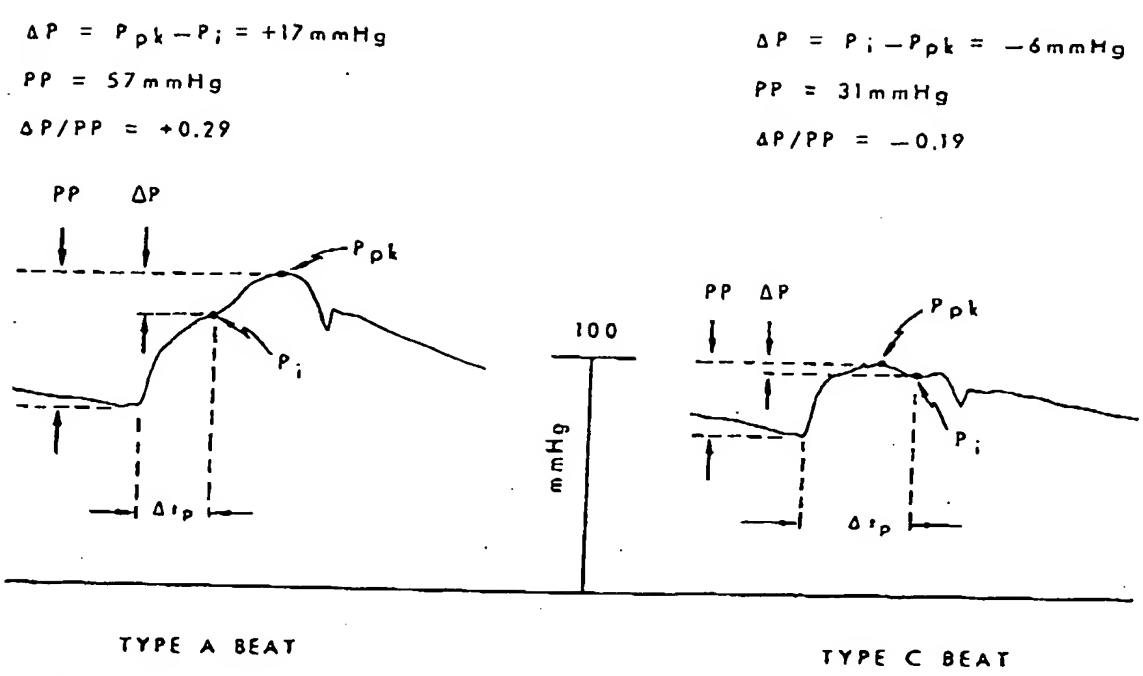

FIGURE 3. *Pressure wave form classification (see text). An example of how the ratio Δ P/PP was calculated is given for both a type A and a type C beat.*

To characterize the patterns of the impedance m duli plots for the three subgroups, each subject's amplitude spectra were normalized to his or her characteristic impedance (Z_c). The normalized moduli and the phases were then averaged by harmonic for each subgroup.

Results

Two of the patients were female and 16 were male. General patient characteristics and hemodynamic data appear in table 1. Although there was a tendency toward decreasing age from group A to group C, a significant difference was present only between group A and group C. There were no significant differences in cardiac output, cardiac index (not tabulated), peak aortic flow or aortic pressure among groups A, B and C.

Examples of the impedance spectra obtained from a patient with type A beats and a patient with type C beats are shown in figure 4. In both patients, the amplitude spectra for the aortic input impedance display a relatively large mean term (the peripheral resistance) with a rapid fall within several Hz to an average or characteristic impedance (Z_c) of 1/10 to 1/20 of the peripheral resistance. The phase angle is negative at low frequencies and becomes positive or zero at the higher harmonics. The initial zero crossing of the phase angle occurs near the same frequency as the first minimum of the amplitude spectrum. Despite these similarities, a distinct difference in the amplitude spectra of the two patients illustrated in figure 4 is evident. The pattern of the modulus spectrum for the patient with the type A beats demonstrates a very distinct minimum at the third harmonic, followed by a distinct maximum at the sixth harmonic. However, the patient with type C beats demonstrates a flatter spectrum in the first six harmonics. The patient with type A beats also demonstrates a more negative phase angle at the lower harmonics.

Patients were grouped by the magnitude of ΔP/PP because this was an obvious differentiating factor based on the pressure wave forms (fig. 3 and table 2). Figure 5 illustrates the average impedance spectra for each subgroup after normalization to characteristic impedance. Although averaging by harmonics may cause smoothing of spectra if heart rates and patient size vary considerably,[22] such an average serves to compact the data for groups of patients and so was used to examine the patterns of the spectral plots for the three groups. When so organized, the differences among the subgroups were found to be similar to the individual examples shown in figure 4. Patients in group A demonstrated well-defined minima and maxima and relatively large oscillations about Z_c, while those in group C revealed a flat or less well organized amplitude spectrum. Group B demonstrated an intermediate pattern. These differences in the patterns of the impedance spectral plots are noteworthy because no significant differences in peripheral resistance or characteristic impedance were found among the three subgroups (table 3). The average peripheral resistance for the entire group was 1137 dyn-sec-cm^{-5} and the average characteristic impedance was 47 dyn-sec-cm^{-5}. These results are similar to those reported by Nichols et al.,[5] but the characteristic impedance in these normal patients is lower than that reported by others.[4-7, 9]

Foot-to-foot pulse-wave velocity measurements are given in table 2. The foot-to-foot pulse-wave velocity

TABLE 1. *Patient Characteristics and Hemodynamic Data*

Pt	Age (years), sex	BSA (m^2)	Aortic radius (cm)	Heart rate (beats/min)	Pressure data: Ao S (mm Hg)	Ao D (mm Hg)	Ao M (mm Hg)	Flow data: Cardiac output (l/min)	Stroke volume (ml)	Peak flow (ml/sec)
Group A (n = 7)										
A1	54 F	1.86	1.4	78	126	68	96	6.7	86	655
A2	53 F	2.00	1.5	69	146	73	104	6.8	99	622
A3	38 M	2.02	1.1	66	111	71	91	7.1	109	750
A4	32 M	1.97	1.1	59	109	70	85	6.6	112	879
A5	35 M	1.96	1.3	68	111	71	90	6.8	100	560
A6	32 M	1.88	1.0	79	120	82	99	6.7	85	698
A7	39 M	2.07	1.3	63	124	73	95	5.7	91	775
Mean ± SEM	40 ± 4*	1.97 ± 0.03	1.2 ± 0.1	69 ± 3	121 ± 5	73 ± 2	95 ± 2	6.6 ± 0.2	97 ± 4	706 ± 40
Group B (n = 7)										
B1	24 M	1.58	1.3	81	115	82	99	4.9	61	464
B2	43 M	1.86	1.4	92	110	79	94	7.7	84	757
B3	33 M	2.00	1.2	66	107	76	92	7.1	108	786
B4	37 M	1.98	1.1	59	101	64	82	6.1	104	787
B5	25 M	2.09	1.0	94	125	89	108	7.1	76	745
B6	38 M	2.13	1.3	110	125	94	109	7.9	72	557
B7	30 M	2.06	1.4	71	108	74	92	6.4	90	589
Mean ± SEM	33 ± 3	1.96 ± 0.07	1.2 ± 0.1	82 ± 7	113 ± 3	80 ± 4	97 ± 4	6.7 ± 0.4	85 ± 6	669 ± 49
Group C (n = 4)										
C1	23 M	2.19	1.1	65	111	84	97	7.1	109	835
C2	29 M	2.04	1.2	80	100	70	87	8.2	102	626
C3	19 M	1.87	1.3	85	126	89	109	6.9	81	586
C4	25 M	2.14	1.3	88	129	79	102	7.7	88	638
Mean ± SEM	24 ± 2*	2.06 ± 0.07	1.2 ± 0.1	80 ± 5	116 ± 7	80 ± 4	99 ± 5	7.5 ± 0.3	95 ± 6	671 ± 56
Total (n = 18)										
Mean ± SEM	34 ± 2	1.98 ± 0.03	1.2 ± 0.03	76 ± 3	117 ± 3	77 ± 2	96 ± 2	6.9 ± 0.2	92 ± 3	684 ± 26

*$p < 0.05$, analysis of variance with Scheffe's test for multiple comparison (Scheffe[25]).
Abbreviations: BSA = body surface area; Ao S, D, M = aortic systolic, diastolic and mean pressures.

is close to the true phase velocity (c) and to the average apparent phase velocity above 2 Hz.[2] The foot-to-foot pulse-wave velocity averaged over all patients was 6.68 m/sec, which is similar to the results reported by Learoyd and Taylor[23] and close to the average apparent phase velocity above 2 Hz as published by Gabe et al.[6] Except for patient C-3, there was a tendency toward lower pulse-wave velocities in the younger age group.

The simplest analog model that displays many of the features of the impedance data described above is an elastic tube connected to a pump and terminated in a resistance.[2, 7, 24] When the terminating resistance differs from the characteristic impedance of the tube, wave reflections arise at the termination of the tube and result in a pattern of minima and maxima in the modulus of the input impedance associated with zero crossings of the phase angle. If, for the purposes of conceptualization, one applies this simple model to the aorta, it is possible to derive an "effective" length, i.e., the distance from measurement site to reflection site, by the quarter wave length relationship[7]:

$$L_e = c/(4f_{min}) \quad (1)$$

where L_e is the effective length, c is the phase velocity, and f_{min} is the frequency at which the first minimum of the impedance modulus occurs. Using the foot-to-foot pulse-wave velocity as an approximation to the phase velocity,[2, 6] L_e may be expressed as:

$$L_e = PWV/(4f_{min}) \quad (2)$$

This relationship was used to calculate the "effective" length of the arterial system and found to be similar in all three groups (table 3) with an average

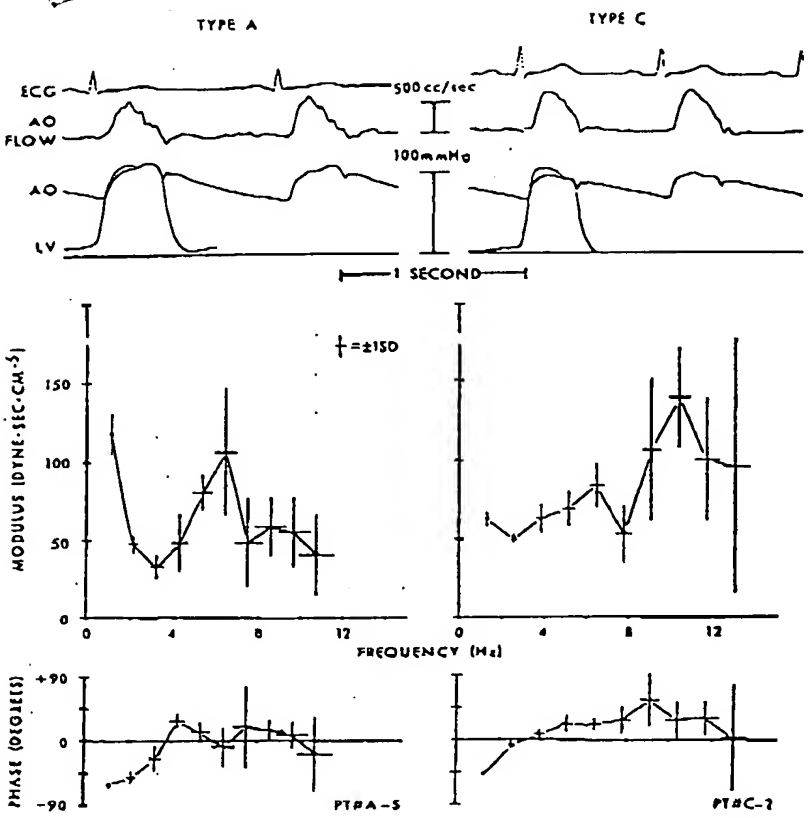

FIGURE 4. *Pressure and flow waves and corresponding impedance plots from type A and type C beats. The zero-Hz term of the impedance (peripheral resistance) is 1059 ± 26 dyn-sec-cm^{-5} (± SD) for patient A-5 and 849 ± 59 dyn-sec-cm^{-5} for patient C-2. AO = aortic; LV = left ventricular.*

distance of 44 ± 2 cm (± SEM).

If the terminating resistance in the single tube model is more closely matched to the tube's characteristic impedance, wave reflections will be minimal or absent and the impedance spectrum is "flatter."

An indicator of the amplitude of oscillation of the impedance moduli about the characteristic impedance (and therefore of the degree of arterial reflection[2]) is given by the equation:

$$(Z_{max} - Z_{min})/Z_c \qquad (3)$$

where Z_{min} and Z_{max} are the values of the minimum and maximum input impedance moduli. There is a

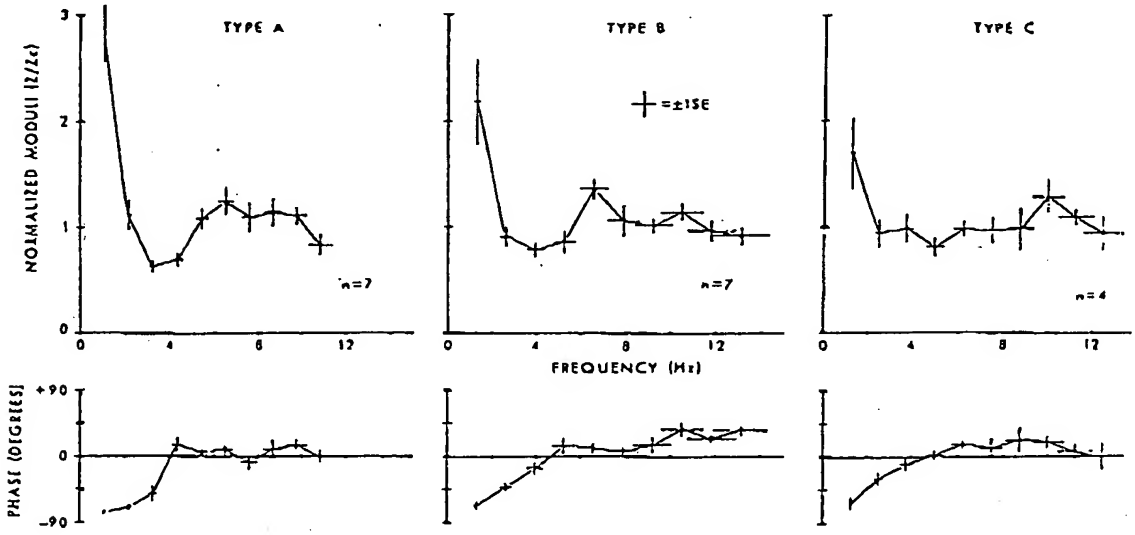

FIGURE 5. *Average normalized impedance spectra for the three subgroups.*

TABLE 2. *Data Derived from Pressure Wave Forms*

Pt	ΔP/PP	Δt_p (msec)	L_p (cm)	PWV (m/sec)
Group A (n = 7)				
A1	0.32	106	33	6.31
A2	0.38	113	49	8.66
A3	0.18	135	48	7.15
A4	0.15	155	56	7.22
A5	0.19	150	50	6.71
A6	0.24	130	31	4.82
A7	0.18	160	53	6.59
Mean ±SEM	0.23 ±0.03	136 ± 8	46 ± 4	6.78 ±0.44
Group B (n = 7)				
B1	0.10	160	51	6.42
B2	0.11	108	32	5.92
B3	0.09	188	55	5.81
B4	0.10	179	59	6.63
B5	0.00	145	34	4.64
B6	0.05	125	53	8.42
B7	0.12	173	65	7.57
Mean ±SEM	0.08 ±0.02	154 ± 11	50 ± 5	6.49 ±0.47
Group C (n = 4)				
C1	−0.12	189	54	5.70
C2	−0.13	180	50	5.52
C3	−0.06	109(176)*	51(83)*	9.45
C4	−0.09	173	—*	—*
Mean ±SEM	−0.10 ±0.02	163 ± 18	52 ± 2	6.89 ±1.28
Total (n = 18)				
Mean ±SEM	0.10 ±0.03	149 ± 7	48 ± 2	6.68 ±0.32

*See text.

Abbreviations: ΔP/PP—see figure 3; Δt_p—see figure 3; L_p = effective reflection distance (see text); PWV = pulse-wave velocity.

significant difference in this expression between the subgroups A and C (table 3).

Since more oscillatory spectra were associated with type A beats and flatter spectra with type C beats, the secondary rise in systolic pressure may well be due to reflected waves from the "effective" reflection site in the arterial system. The more pronounced secondary rise in systolic pressure found in type A beats and the less prominent late systolic characteristics of the type C beat may simply be a result of differences in timing and magnitude of reflections.

To investigate this further, an attempt to derive the effective reflection site distance from the pressure wave form alone was made using the relationship[23]:

$$L_p = PWV\ \Delta t_p/2 \qquad (4)$$

where L_p is the effective length and Δt_p (defined in figure 3) represents the time of travel of the wave from the heart to the reflection site and back. If the single uniform tube model can be used as a first approximation of the aorta, then the distances L_z and L_p should be equal.

The average distance for the three groups calculated by equation 4 (L_p) was 48 ± 2 cm (see table 2), which is very close to the value found by equation 2 (L_z). Again, no significant difference was found among subgroups.

Figure 6A demonstrates the relationship derived from the data shown in tables 2 and 3. (Patient C-3 seemed to have two reflections, which appeared in both the pressure wave form and the impedance spectra; the modulus spectrum for patient C-4 was so flat that no f_{min} or f_{max} could be measured.) A linear relationship can be seen, but with a tendency toward "clumping" of the data at a length of 44–48 cm.

The calculation of an effective length from the pressure pulse itself (L_p) correlates well with calculation of the effective length from the impedance spectra (L_z). Equations 2 and 4 may then be used to derive the relationship

$$\Delta t_p = 1/(2f_{min}) \qquad (5)$$

where $1/2f_{min}$ has the dimension of time and may be expressed as Δt_z. The relationship between transit time derived from the pressure data (Δt_p) and transit time derived from the impedance data (Δt_z) is shown in figure 6B. A linear relationship is again demonstrated, with less clumping effect than in figure 6A.

Discussion

This study demonstrates that input impedance can be obtained without additional risks to the patient if new methods such as the multisensor techniques described here are used. Impedance should be determined for a series of beats in the steady state rather than from a single beat, because beat-to-beat variations due to noise may be considerable (fig. 2). Spectra from 10 beats are suggested as the minimum number to be averaged for reliable results. This study has established the normal ranges of input impedance values in adult man (table 3).

The pressure wave forms were divided into three subgroups (A, B and C; fig. 3) and related to the impedance spectral patterns. The impedance spectra for type A beats reveal an oscillatory behavior that suggests considerable reflection in the arterial system.[2, 22, 24] The impedance plots derived from the type C beats demonstrate flatter spectra, implying smaller or more diffuse reflections. The type B beats are intermediate between these two. Another expression of the amount of reflection in the system is the magnitude of the first harmonic of the normalized impedance moduli.[22] In figure 5, the amplitude of the first harmonic of the normalized impedance moduli is highest in group A patients, lowest in group C patients and intermediate in group B patients. The difference between the group A and group B patients may be partly due to the lower frequency of the fundamental harmonic in group A (1.1 Hz) compared with group B (1.3 Hz). However, in group C patients, the fun-

TABLE 3. *Data Derived from Impedance Spectra*

Patient	R_p*	Z_o*	$\frac{Z_{max}-Z_{min}}{Z_o}$	f_s (Hz)	f_{min} (Hz)	f_{max} (Hz)	L_s (cm)
Group A (n = 7)							
A1	1146	56	1.04	5.0	5.0	9.0	32
A2	1223	76	1.45	4.0	4.4	8.8	49
A3	1025	47	0.94	3.5	3.5	6.0	51
A4	1066	34	0.83	4.5	3.8	6.3	48
A5	1059	53	1.26	3.5	3.3	6.6	51
A6	1182	39	0.92	4.2	3.6	5.0	33
A7	1333	37	0.57	4.0	3.5	6.0	47
Mean ± SEM	1148 ± 41	49 ± 6	1.00 ± 0.11†	4.1 ± 0.2	3.9 ± 0.2	6.8 ± 0.6	44 ± 3
Group B (n = 7)							
B1	1616	71	0.54	4.1	3.9	6.5	41
B2	976	29	1.21	4.8	5.0	7.0	30
B3	1036	31	0.55	4.2	3.3	6.0	44
B4	1075	31	0.28	6.6	3.7	5.6	45
B5	1217	37	0.62	6.5	4.5	7.5	26
B6	1104	65	0.98	4.5	4.4	8.0	48
B7	1150	52	0.82	4.8	3.3	6.6	57
Mean ± SEM	1168 ± 80	45 ± 7	0.71 ± 0.12	5.1 ± 0.4	4.0 ± 0.2	6.7 ± 0.3	42 ± 4
Group C (n = 4)							
C1	1093	30	0.44	3.5	3.0	6.0	48
C2	849	58	0.12	3.5	2.6	6.0	50
C3	1263	39	0.70	4.5	5.6(2.8)‡	10.0	42(88)‡
C4	1059	62	0.15	—‡	—‡	—‡	—‡
Mean ± SEM	1066 ± 85	47 ± 8	0.36 ± 0.14†	3.8 ± 0.3	3.7 ± 0.9	7.3 ± 1.3	47 ± 2
Total (n = 18)							
Mean ± SEM	1137 ± 39	47 ± 4	0.74 ± 0.09	4.5 ± 0.2	3.9 ± 0.2	6.9 ± 0.3	44 ± 2

*All impedance parameters are in dyn-sec-cm^{-5}.
†$p < 0.05$, analysis of variance with Scheffe's test for multiple comparison (Scheffe[29]).
‡See text.
Abbreviations: R_p = peripheral resistance (DC component of impedance); Z_{min} = value of first minimum of impedance modulus; Z_{max} = value of maximum of impedance modulus after first minimum; f_s = frequency where first zero crossing of phase occurs; f_{min} = frequency of first minimum of the impedance modulus; f_{max} = frequency of first maximum of the impedance modulus; L_s = effective reflection distance (see text).

damental harmonic has a frequency similar to that of group B patients, but the modulus has a lower amplitude, indicating less influence of reflected waves. Examination of the phase spectra also yields information related to the influence of reflections. In a system without reflections, the phase angle would be close to zero. In the patients with type A beats, the phase angle is much more negative for the first few harmonics than in the other two subgroups.

These results indicate that the secondary rise in the aortic pressure wave is primarily the result of a less well matched arterial system, i.e., a system with considerable reflection, and not secondary to cardiac function. The type A beats, related to an arterial system with large reflections, show a secondary rise in pressure with a tendency toward a larger pulse pressure. The type C beats are present in the system with little or more diffuse reflections, show small secondary rises in pressure and tend toward smaller pulse pressures. The magnitude of the secondary rise in the pressure wave forms appears to be directly related to the magnitude of the oscillations in the impedance spectra.

Among the three subgroups there were no significant differences in mean aortic pressure, aortic radius, characteristic impedance and pulse-wave velocity (tables 1, 2 and 3). The ascending aortic properties are therefore expected to be similar in these patients. The arterial systems at the arteriolar level also appear to be similar; there are no significant differences in peripheral resistance among the groups (table 3). However, the lack of significant differences in these measurements should be approached with some caution due to the small group sizes. The only significant difference found among the three subgroups of patients was age, with type A beats associated with

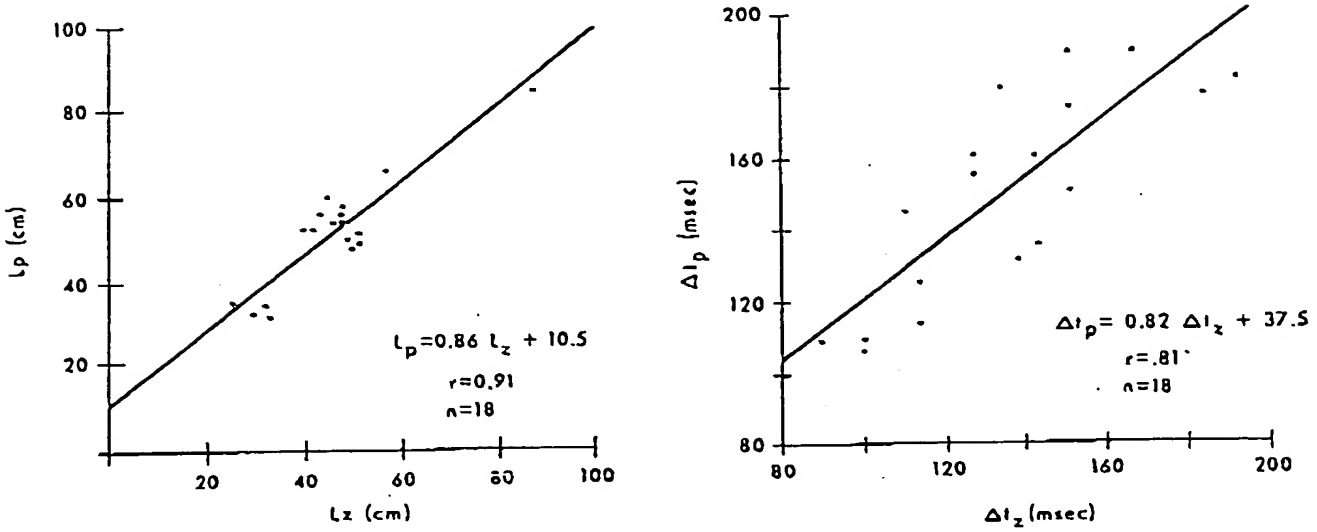

FIGURE 6. *(left) Effective length calculated from the aortic pressure wave (L_p) vs effective length calculated from the frequency of the first minimum of the impedance modulus (L_z). (right) Transit time from pressure data Δt_p (defined in figure 3) vs transit time from impedance data Δt_z (see text).*

older patients and type C beats with younger patients. Impedance mismatch may therefore increase with age. This observation is of interest in two other aspects. First, the greater number of patients with type A and B beats in this study is a reflection that most patients coming to cardiac catheterization are older. Second, aortic input impedance derived from experimental studies in animals generally shows less oscillation about the characteristic impedance than in man.[3, 24, 26] These differences may be explained by the physiologically younger ages of the experimental animals compared to the majority of human subjects (subgroups A and B) reported in this study and in patients with cardiovascular disease.[4–9]

The location in the arterial system from which such reflections arise was examined using data derived from both the impedance spectra and the pressure wave forms (equations 2 and 4). In most patients, the distance to the effective reflection site (the effective length of the system) was 44–48 cm from the ascending aorta. In the adult population studied, this distance approximates the region of the terminal abdominal aorta and bifurcation into the iliac and femoral arteries. Mills et al.[7] also found an average distance of 44 cm in five patients using f_{min}. Although it is tempting to conclude that this represents a single reflection site, other investigators[22, 24, 25] have shown that reflections in the arterial system arise from many points. In a model study, Sipkema and Westerhof[27] demonstrated that the assumption of a single reflection may lead to errors. The impedance spectra derived in these studies are not identical to those derived from a single uniform tube model; the arterial system is more complex.[2, 24] However, in the archetypal ascending aortic pressure pulse of adult man, a well-defined single inflection point is almost always present. This is in contradistinction to most pressure wave forms in laboratory animal experiments where major interventions, such as the inflation of an intraaortic balloon,[23] are required to produce wave forms similar to the type A and type B beats described in the present study. Thus, although reflections occur from multiple locations in the arterial system, it appears that the region of the terminal abdominal aorta generates reflections that dominate over those arising from other locations in man. We have therefore chosen to use the term "effective" reflective site.

O'Rourke and Taylor[22] analyzed the impedance spectra in dogs and concluded that reflections result from two major sites in the arterial system. These spectra appear to correlate better with an eccentric T-tube model,[28] in which the shorter tube corresponds to the vessels in the upper part of the body and the longer tube represents the vasculature in the lower part of the body. Reflections in the longer tube give rise to minima of the impedance moduli at the lower frequencies, but reflections in the upper tube would give rise to a second minimum at the higher frequencies. These characteristics might also give rise to two inflection points in the pressure wave form, with the first inflection a result of a reflection from the cephalad tube and the second a result of a reflection from the caudal tube. Although this model may be a more realistic approximation of the arterial system, the ranges f normal heart rates in man do not allow a reliable evaluation of minima and maxima points in the higher frequencies due to signal noise. Furthermore, an early inflection point in the ascending aortic pressure wave form is rarely seen in normal man. In two or three patients in this study such an inflection point was suggested and appeared to correlate to a second minimum point in the impedance spectra. However, most patients do not demonstrate such a finding, and the major reflection appears to come from the terminal abdominal aorta.

To pursue this point further, the change in the shape

of the aortic pressure wave as it travels from the ascending aorta to the terminal abdominal aorta is shown in figure 7 in one patient with a type A beat. The appearance of the reflected wave, as indicated by the timing of the inflection point, occurs progressively earlier in systole as the wave approaches the iliac bifurcation. We consider the early diastolic wave in the ascending aorta (denoted by arrows in figure 7) as part of this reflected wave. As the initial portion of the reflected wave progresses towards early systole with increasing distance from the aortic valve, the diastolic or trailing portion of the reflected wave moves from diastole into systole. This is in contrast to the explanation for the change in aortic pressure contour suggested by O'Rourke,[28] where the reflection appeared to move progressively later into systole. In addition to the earlier appearance of the reflected wave, the amplitude of the reflection increases peripherally. The lines connecting the initial aortic upstroke and the onset of the secondary pressure rise in figure 7 approach each other as pressure is measured in the terminal abdominal aorta. These observations further support the evidence that this region behaves as the major reflection site in man.

An increase in the magnitude of reflections was attempted by bilateral external compression of the femoral arteries in four patients; one is shown in figure 8. This intervention immediately produces a change in the ascending aortic pressure wave form. In this example, the end-diastolic pressure and the pressure at the inflection point do not change significantly, but the late systolic portion of the ascending aortic wave form immediately increases. The preocclusion value for ΔP (defined in figure 3) was 10 mm Hg and increased to 20 mm Hg in the beat immediately after occlusion. The total change in aortic pulse pressure is solely accounted for by this change in the late secondary rise in aortic pressure. An augmentation of reflection phenomena was thus accomplished by external occlusion of vessels in the region of the effective reflection site.

Although an analysis of the pressure wave form itself does yield information regarding the arterial system, especially with regard to the presence or absence of reflections, it should be emphasized that pressure and flow depend not only on the arterial load, but also on the pump function of the heart. In this study, the differences in wave forms were associated with differences in the arterial system as demonstrated by input impedance calculations, but no significant differences in cardiac function were found.

This study has demonstrated the ability to measure in a clinical cardiovascular laboratory simultaneous pressure and flow wave forms in man in order to calculate ascending aortic input impedance. The average of more than 15 beats per patient in a group of 18 patients without any evidence of organic heart disease has established the normal range of input im-

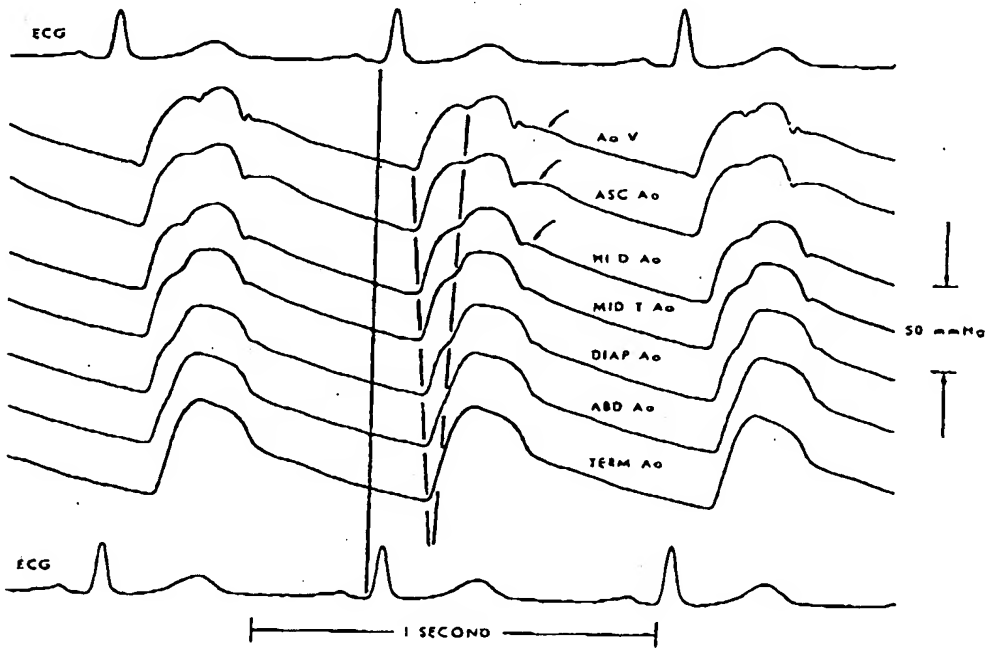

FIGURE 7. *Pressure wave forms as a function of location from the ascending aorta to the iliac bifurcation in one patient. Figure constructed from single or pairs of pulses selected from cardiac cycles with equal RR intervals and from similar phases of respiration. Ao V = sensor just above aortic valve; Asc Ao = ascending aorta; Hi D.Ao = high descending aorta; Mid T.Ao = midthoracic aorta; Diap Ao = diaphragmatic aorta; Abd Ao = abdominal aorta; Term Ao = terminal abdominal aorta just before iliac bifurcation. See text for discussion.*

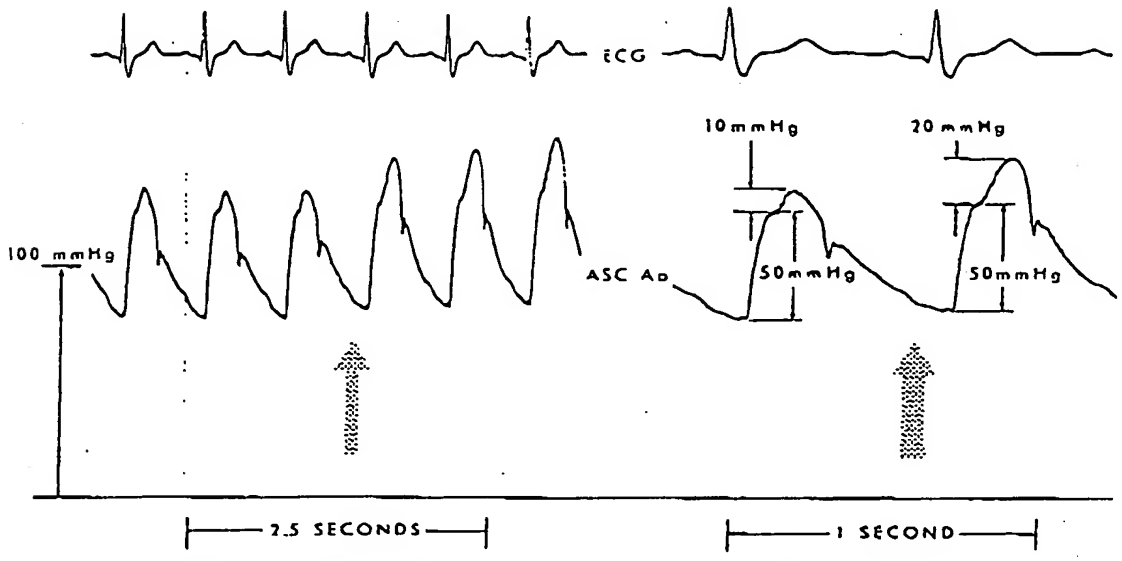

FIGURE 8. *Ascending aortic (Asc A.) pressure wave forms pre- and post-bilateral occlusion of the femoral arteries by external manual compression. (left) Slow-speed recording demonstrating immediate increase in systolic pressure from 139 mm Hg to 153 mm Hg after compression (denoted by arrow). (right) Higher speed recording of the pre- and postocclusion beats. The diastolic aortic pressure has increased only 4 mm Hg as a result of decreased peripheral runoff. The initial portion of the aortic-pulse pressure from upstroke to the inflection point remains unchanged at 50 mm Hg. The secondary rise in late systolic pressure (ΔP) increases from 10 mm Hg to 20 mm Hg. The reflected wave has increased by 100% and forms the major contribution to the total increase in systolic pressure.*

pedance data. The differences in impedance spectral plots were correlated to the differences in the ascending aortic pressure wave forms. These differences were related to the magnitude of the reflections and the effective length of the arterial system. Although reflections occur from many sites in the arterial tree, the major effective reflection site in man appears to be the region of the terminal abdominal aorta.

Acknowledgment

The authors gratefully acknowledge the invaluable assistance of Thomas Dunne and the technicians of the Cardiac Catheterization Laboratory at Brooke Army Medical Center, SP5 Thomas R. Deojay and James W. Bagwell for their assistance in data processing. Dr. Barry R. Alter and the physicians of the Cardiology Service for their cooperation and Bettye Jo Hairston for her outstanding assistance in typing this manuscript. The photography and graphics were provided by Earl Ferris, SP5 David Lovelace, SP5 Georgette Toshok, and Douglas Meyer.

References

1. Murgo JP, Altobelli SA, Dorethy JF, Logsdon JR, McGranathan GM: Normal ventricular ejection dynamics in man during rest and exercise. *In* Physiologic Principles of Heart Sounds and Murmurs, edited by Leon DF, Shaver JA. Dallas, American Heart Association, 1975, p 92
2. McDonald DA: Blood Flow in Arteries, Baltimore, Williams and Wilkins, 1974
3. Westerhof N, Murgo JP, Sipkema P, Giolma JP, Elzinga G: Arterial impedance. *In* Quantitative Cardiovascular Studies edited by Hwang NHC, Gross DR, Patel DJ. Baltimore, University Park Press, 1979, p 111
4. Patel DJ, Austen WG, Greenfield JC: Impedance of certain large blood vessels in man. Ann NY Acad Sci 115: 1129, 1964
5. Patel DJ, Greenfield JC, Austen WG, Morrow AG, Fry DL: Pressure-flow relationships in the ascending aorta and femoral artery in man. J Appl Physiol 20: 459, 1965
6. Gabe IT, Karnell IG, Rudewald B: The measurement of input impedance and apparent phase velocity in the human aorta. Acta Physiol Scand 61: 73, 1964
7. Mills CJ, Gabe IT, Gault JH, Mason DT, Ross J Jr, Braunwald E, Shillingford JP: Pressure flow relationships and vascular impedance in man. Cardiovasc Res 4: 405, 1970
8. Nichols WW, Conti CR, Walker WE, Milnor WR: Input impedance of the systemic circulation in man. Circ Res 40: 451, 1977
9. Pepine CJ, Nichols WW, Conti CR: Aortic input impedance in heart failure, Circulation 58: 460, 1978
10. Cohn JN: Vasodilator therapy for heart failure: the influence of impedance on left ventricular performance. Circulation 48: 5, 1973
11. Ross J Jr: Afterload mismatch and preload reserve: a conceptual framework for the analysis of ventricular function. Prog Cardiovasc Dis 18: 255, 1976
12. Shah PK: Ventricular unloading in the management of heart disease: role of vasodilators, parts I and II. Am Heart J 93: 256, 403, 1977
13. Chatterjee K, Parmley W: The role of vasodilator therapy in heart failure. Prog Cardiovasc Dis 19: 301, 1977
14. Milnor WR: Arterial impedance as ventricular afterload. Circ Res 36: 565, 1975
15. Noble MIM: Left ventricular load, arterial impedance and their interrelationship. Cardiovasc Res 13: 183, 1979
16. Murgo JP, Millar H: A new cardiac catheter for high fidelity differential pressure recordings. *In* Proc 25 Ann Conf Eng Med Biol, Bell Harbour, Fla, 1972, (abstr) p 303
17. Murgo JP: New techniques in cardiac catheterization: the advantages of multisensor catheters. *In* Proc Int Conf Biomed Transducers, Paris, 1975, p 41
18. Murgo JP, Giolma JP, Altobelli SA: Signal acquisition and processing for human hemodynamic research. *In* Proc IEEE 65: 696, 1977

19. Slonin N, Bell B, Christensen S: Cardiopulmonary Laboratory Basic Methods and Techniques. Springfield, Ill. Charles C Thomas, 1967, p 124
20. Murgo JP: Multisensor cardiac catheterization. New methods to study cardiovascular dynamics in man. *In* Proc 28 Ann Conf Eng Med and Biol, New Orleans, 1975, (abstr) p 503
21. Schultz DL, Tunstall-Pedoe DS, Lee G. de J, Gunning AJ, and Bellhouse BJ: Velocity distributions and transition in the arterial system. *In* Ciba Symposium on Circulation and Resp. Mass Transport, edited by Wolstenholme GEW, Knight J. London, Churchill-Livingston, 1969, p 172
22. O'Rourke MF, Taylor MG: Input impedance of the systemic circulation. Circ Res 20: 365, 1967
23. Learoyd BM, Taylor MG: Alterations with age in the viscoelastic properties of human arterial walls. Circ Res 18: 278, 1966
24. Westerhof N, Elzinga G, van den Bos GC: Influence of central and peripheral changes on the hydraulic input impedance of the systemic arterial tree. Med Biol Eng 11: 710, 1973
25. van den Bos GC, Westerhof N, Elzinga G, Sipkema P: Reflection in the systemic arterial system: effects of aortic and carotid occlusion. Cardiovasc Res 10: 565, 1976
26. Noble, MIM, Gabe IT, Trenchard D, Guz A: Blood pressure and flow in the ascending aorta of conscious dogs. Cardiovasc Res 1: 9, 1967
27. Sipkema P, Westerhof N: Effective length of the arterial system. Ann Biomed Eng 3: 296, 1975
28. O'Rourke MF, Cartmill TB: Influence of aortic coarctation on pulsatile hemodynamics in the proximal aorta. Circulation 44: 281, 1971
29. Scheffé H: A method of judging all contrasts in the analysis of variance. Biometrika 40: 87, 1953

Contractile Performance of the Hypertrophied Ventricle in Patients with Systemic Hypertension

MASAAKI TAKAHASHI, M.D., SHIGETAKE SASAYAMA, M.D., CHUICHI KAWAI, M.D., AND HAJIME KOTOURA, M.D.

SUMMARY **To assess the contractile state of the hypertrophied ventricle induced by long-standing systemic hypertension in 22 patients, we used echocardiography for the measurement of the ventricular diameter and posterior wall thickness, together with simultaneous recording of brachial arterial pressure. Meridional wall stress (WSt) was used for the expression of the force per unit cross-sectional area. The WSt–diameter relation obtained during dynamic responses to acute pressure reduction by nitroprusside infusion was compared with the same relation obtained in 10 normal subjects (posterior wall thickness averaged 0.7 cm [range 0.6–0.9 cm]) over a range of matched systolic pressure induced by methoxamine administration. In 15 patients in whom end-diastolic wall thickness increased to 1.1 cm (range 1.0–1.2 cm), the linear WSt–diameter relation at end-systole did not differ from the control group, indicating a normal level of inotropic state. In the seven patients with an end-diastolic wall thickness of 1.3 cm or more, the end-systolic WSt–diameter relation was clearly shifted to the right and had a less steep slope. These findings indicate that in advanced left ventricular hypertrophy induced by pressure overload, myocardial contractility may be depressed.**

CARDIAC HYPERTROPHY is one of the fundamental mechanisms of adaptation to abnormal loading conditions; however, the effects of hypertrophy on myocardial performance are controversial. Although initial studies of severe pressure overload on the cat right ventricle demonstrated depressed function,[1-3] more recent studies in similar preparations indicated a gradual improvement of the contractile state during subsequent weeks, thereby emphasizing the important temporal relationship between the inotropic state level and the degree and duration of loading.[4]

Sasayama and colleagues developed an experimental model for chronic pressure overloading by aortic constriction of conscious dogs and serially assessed the ventricular function over several weeks.[5] They found that the left ventricle responded to chronically elevated pressure by initial dilatation with increased wall stress and then gradual development of hypertrophy with a consequent reduction in wall stress to near-normal states. Wall stress–diameter loops during a single contraction were then analyzed over a range of matched systolic pressures during acute aortic constriction before and after induction of chronic hypertrophy produced by sustained aortic constriction. The linear relation between left ventricular (LV) diameter and wall stress at the end of ventricular ejection was the same in control and hypertrophied hearts.[6] They concluded that in successful adaptation to the pressure overload, hypertrophy per se did not produce intrinsic depression of the myocardial inotropic state.[6] However, these experimental overloads were acutely in-

From the Third Division, Department of Internal Medicine, and the Central Clinical Laboratory, Faculty of Medicine, Kyoto University, Kyoto, Japan.

Supported by Scientific Research Grant 244044 from the Ministry of Education, Science and Culture, Tokyo, Japan.

Presented in part at the 28th Annual Scientific Sessions of the American College of Cardiology, Miami Beach, Florida, March 1979.

Address for correspondence: Chuichi Kawai, M.D., The Third Division, Department of Internal Medicine, Faculty of Medicine, Kyoto University, Shogoin, Sakyo-ku, Kyoto 606, Japan.

Received June 28, 1979; revision accepted January 5, 1980.
Circulation 62, No. 1, 1980.